The role of the diencephalon in the guidance of thalamocortical axons in mice

Idoia Quintana-Urzainqui[1], Pablo Hernández-Malmierca P[2,3], James M. Clegg[1], Ziwen Li[4], David J Price[1]

[1] Centre for Discovery Brain Sciences, Hugh Robson Building, George Square, Edinburgh EH8 9XD, United Kingdom

[2] Heidelberg Institute for Stem Cell Technology and Experimental Medicine (HI-STEM gGmbH), 69120 Heidelberg, Germany

[3] Division of Stem Cells and Cancer, Deutsches Krebsforschungszentrum (DKFZ) and DKFZ-ZMBH Alliance, 69120 Heidelberg, Germany

[4] Centre for Cardiovascular Science, Queen's Medical Research Institute, 47 Little France Crescent, Edinburgh EH16 4TJ, United Kingdom

Corresponding author address: idoia.quintana@ed.ac.uk

Key words (3-6)

Thalamocortical tract, axon guidance, diencephalon, Pax6, thalamus, prethalamic pioneer axons.

Abstract

Thalamocortical axons (TCAs) cross several tissues on their journey to the cortex. Mechanisms must be in place along the route to ensure they connect with their targets in an orderly fashion. The ventral telencephalon acts as an instructive tissue, but the importance of the diencephalon in TCA mapping is unknown. We report that disruption of diencephalic development by Pax6 deletion results in a thalamocortical projection containing mapping errors. We used conditional mutagenesis to test whether these errors are due to the disruption of pioneer projections from prethalamus to thalamus and found that, while this causes abnormal TCA fasciculation, it does not induce topographical errors. To test whether the thalamus contains important navigational cues for TCAs, we used slice culture transplants and gene expression studies. We found the thalamic environment is instructive for TCA navigation and that the molecular cues Netrin1 and Semaphorin3a are likely to be involved. Our findings indicate that the correct topographic mapping of TCAs onto the cortex requires the order to be established from the earliest stages of their growth by molecular cues in the thalamus itself.

Introduction

A striking feature of the axonal tracts that interlink the nervous system's component parts is the high degree of order with which they map the array of neurons in one structure onto the array of neurons in their target. Often, the order of axons at the target closely mirrors that at the source. An excellent example is the mapping of thalamic neurons onto their cerebral cortical targets via the thalamocortical pathway (Fig. 1A). Thalamic neurons located at one end of the thalamus in a dorsolateral region called the dorsal lateral geniculate nucleus (dLGN) innervate the caudal (visual) part of cortex; neurons located at the other end of the thalamus in more rostral-medial regions known as the ventrolateral (VL) and ventromedial (VM) nuclei innervate more rostral cortical regions, including motor and frontal cortex; neurons located in between - in the ventromedial posterior (VMP) nuclei - innervate central (somatosensory) cortex (Fig. 1A) (Amassian and Weiner, 1966; Bosch-Bouju et al., 2013; Jones, 2007; Tlamsa and Brumberg, 2010). The mechanisms that generate this orderly topographic mapping remain poorly understood.

The maintenance of order among thalamic axons as they grow is likely to contribute to the generation of orderly topographic mapping in the mature thalamocortical tract. During embryogenesis, thalamic axons exit the thalamus from about E12.5 onwards (Auladell and Hans, 2000; Braisted et al., 1999; Tuttle et al., 1999), approximately coincident with the cessation of neurogenesis in this structure (Angevine, 1970; Li et al., 2018). They then cross the adjacent prethalamus and turn laterally out of the diencephalon and into the ventral telencephalon where they traverse two consecutive instructive regions - the corridor (Lopez-Bendito et al., 2006) and the striatum - before entering the cortex. There is evidence that the maintenance of spatial order among thalamocortical axons (TCAs) crossing the ventral

telencephalon requires interactions between the axons and signals released by cells they encounter in this region (Bielle et al., 2011; Bonnin et al., 2007; Braisted et al., 1999; Dufour et al., 2003; Molnár et al., 2012; Powell et al., 2008). The importance of earlier interactions within the diencephalon remains unclear.

Here, we tested the effects of mutating the gene for the Pax6 transcription factor, which is essential for normal diencephalic patterning (Caballero et al., 2014; Clegg et al., 2015; Parish et al., 2016; Pratt et al., 2000; Stoykova et al., 1996; Warren and Price, 1997), on the topographic mapping of TCAs onto the cortex. Pax6 starts to be expressed in the anterior neural plate well before TCAs start to form (Walther and Gruss, 1991). As the forebrain develops from the anterior neural plate, Pax6 expression becomes localized in (i) cortical progenitors that generate the target neurons for TCAs, (ii) diencephalic (thalamic and prethalamic) progenitors and (iii) prethalamic (but not thalamic) postmitotic neurons (Quintana-Urzainqui et al., 2018; Stoykova et al., 1996; Warren and Price, 1997). We discovered that deletion of Pax6 from mouse embryos at the time when thalamic axons are starting to grow results in the development of a thalamocortical projection containing mapping errors. Axons from dorsolateral thalamus are misrouted medially and end up projecting abnormally rostrally in the cortex. We went on to explore the reasons for this defect.

We first used conditional mutagenesis to test whether misrouting is due to the loss of Pax6 from prethalamic neurons, since previous work has shown that (i) Pax6 is not required in the cortex for normal TCA topography (Piñon et al., 2008) and (ii) Pax6 is neither expressed nor required autonomously by thalamic neurons for them to acquire the ability to extend axons to the cortex (Clegg et al., 2015). We found that while loss of Pax6 from a specific set of prethalamic neurons prevented them developing their normal axonal projections to thalamus and resulted in the abnormal

fasciculation of thalamic axons, it did not cause TCAs to misroute. This suggested that the thalamus itself contains important navigational cues for TCAs. We used slice culture transplants and gene expression studies to show (i) that the thalamic environment is indeed instructive for TCA navigation and (ii) to identify molecular changes within the thalamus that likely cause the disruption in TCA topography observed upon Pax6 deletion. Our findings indicate that the normal topographic mapping of TCAs requires that order be established and maintained from the earliest stages of their growth by molecular cues in the thalamus itself.

Results

Thalamocortical topography is disrupted in *CAG^{CreER}* but not in *Emx^{CreER}* Pax6 conditional knockouts

Previous studies have shown that constitutive loss of Pax6 function causes a total failure of TCA development, which is hypothesized to be a secondary consequence of anatomical disruption at the interface between the diencephalon and the telencephalon (Clegg et al., 2015; Georgala et al., 2011; Jones et al., 2002). No such failure occurs if Pax6 is deleted conditionally after this anatomical link is formed (Clegg et al., 2015). We first assessed whether delayed ubiquitous Pax6 deletion, induced in *CAG$^{CreER\text{-}TM}$ Pax6$^{fl/fl}$* embryos (referred to here as *CAG^{CreER}* Pax6 cKOs), disrupts the topography of TCA connections. We induced Cre recombinase activation by tamoxifen administration at E9.5 which caused Pax6 protein loss in *CAG^{CreER}* Pax6 cKOs from E11.5 onwards (Quintana-Urzainqui et al., 2018), which is when the generation of most thalamic neurons is starting (Li et al., 2018) and before many TCAs have begun to grow (Auladell and Hans, 2000; López-Bendito and Molnár, 2003). We used both wild type and *CAG^{CreER}Pax6$^{fl/+}$* littermate embryos as

controls since the latter express normal levels of Pax6 protein, almost certainly because of a feedback loop that compensates for a deletion in one allele by increasing the activity of the other (Caballero et al., 2014; Manuel et al., 2015).

We inserted two different axonal tracers in two cortical areas in E15.5 fixed brains. DiA was placed in the visual (caudal) cortex while DiI was placed in the somatosensory (more rostral) cortex (Fig. 1B). In controls (both wild type and *Pax6*$^{fl/+}$), DiA retrogradely labelled cells in dorsolateral thalamic areas (dLGN; green labelling in Fig. 1C-F), while DiI labelled cells in ventromedially-located thalamic regions (red labelling in Fig. 1C-F). Labelling of these two thalamic regions was clearly separated in all cases (indicated by dotted line in Fig. 1C-F; n=3 independent replicates for each of the two genotypes). In *CAG*^{CreER} *Pax6* cKOs, however, the two labelled populations overlapped (Fig. 1G-I). In these mutants, the distribution of the DiA-labelled thalamic cells (from caudal cortical injections) was not obviously changed with respect to controls. However, the DiI-labelled cells (projecting to more rostral cortical areas) showed a much wider distribution than in controls and expanded to lateral thalamic areas (compare Fig.1 C-F,C',E'F' versus G-I,H',I'), even overlapping with DiA stained cells at the dLGN (Fig. 1 H',I'). This observation was consistent across three independent experiments, indicating that some TCAs from neurons located at dorsolateral thalamic levels that should project to the caudal cortex are misrouted towards more rostral cortical areas in the *CAG*^{CreER} *Pax6* cKOs (Fig. 1L).

Since Pax6 is expressed both in the cortex and diencephalon during TCA development, the mapping defects described above might have been due to the loss of Pax6 from the cortex. This was unlikely because a previous study showed that Pax6 is not required in the cortex for the establishment of proper topographical

thalamocortical connections (Piñon et al., 2008). To confirm this, we used a cortex-specific, tamoxifen-inducible Cre line (*Emx1*^{CreER}). We administered tamoxifen at E9.5, which results in a near-complete loss of cortical Pax6 between E11.5-12.5 (Georgala et al., 2011; Mi et al., 2013), and performed DiI/DiA labelling at E15.5, following the same experimental design described above for the *CAG*^{Cre} line. We found that the two retrogradely-labelled populations did not overlap in controls (*Emx1*^{CreER} *Pax6*$^{fl/+}$, n=3) or in mutants (*Emx1*^{CreER} *Pax6*$^{fl/fl}$, n=3) (Fig. S1A,B), suggesting that the defects of TCA mapping found in the *CAG*^{CreER} *Pax6* cKOs were not attributable to cortical abnormalities.

To define the anatomical region where thalamic axons probably deviated from ordered growth, we examined the TCA bundle in *CAG*^{CreER}*Pax6* cKOs. This bundle was ordered and segregated into rostral/somatosensory (DiI) and caudal/visual (DiA) halves at its point of exit from the prethalamus and entry into the ventral telencephalon (arrows in Fig. 1 G-I), which indicated that the misrouting of lateral TCAs from dorsolateral thalamus might happen before this point, i.e. within the diencephalon.

TCAs fasciculate prematurely as they cross the prethalamus in *Pax6* conditional mutants

Within the diencephalon, the first structure that thalamic axons encounter as they leave the thalamus is the prethalamus, and its neurons normally express high levels of Pax6. Therefore, we investigated whether the defects of TCA mapping in *CAG*^{CreER} *Pax6* cKOs might arise from a disordered growth of thalamic axons through the prethalamus. As a first step, we examined the effects of Pax6 deletion on the behaviour of thalamic axons as they cross the prethalamus.

Since the neural cell adhesion molecule L1CAM (L1) is expressed in TCAs (Fukuda et al., 1997; Ohyama et al., 2004), we examined the distribution of L1-positive thalamic axons at E13.5 in transverse and sagittal sections through the prethalamus. In controls, axons emerging from the thalamus converge progressively as they cross the prethalamus (Fig. 2A-E) to subsequently form a single thalamocortical bundle that turns laterally and exits the prethalamus (arrows in Fig. 2A,B,E). We found that in *CAG^{CreER} Pax6* cKOs (Fig. 2F-L), thalamic axons prematurely converge into larger bundles as soon as they cross the thalamic-prethalamic boundary (empty arrows in Fig. 2G-I,L).

To obtain a quantitative measurement of this observation we positioned three equally-spaced lines across different diencephalic levels in sagittal sections: (1) at the thalamic-prethalamic border (Th-PTh), guided by prethalamic expression of Pax6; (2) at a lower prethalamic position (low-PTh), guided by the end of Pax6 prethalamic expression; and (3) at the midpoint position between the two other lines (mid-PTh) (lines represented in Fig. 2D,E,K,L). We used Fiji software (Schindelin et al., 2012) to quantify the number of axon bundles crossing each line and the width of each individual bundle. We recognized individual bundles as each single L1-positive structure above a consistent intensity threshold (red lines in Fig. 2M,N). We found a significant decrease in the number of bundles crossing all three checkpoints (Fig. 2O). Axon bundle width strikingly increased at the Th-PTh border and the mid-PTh, with no significant change at the low-PTh checkpoint line (Fig. 2P) (see figure legend for statistical details). These data indicate that, in the absence of Pax6, TCAs begin to fasciculate prematurely in their route, forming bigger and fewer bundles as they cross the prethalamus (Fig. 2Q). We next tested the role of the prethalamus in TCA formation and the potential establishment of their topography.

Prethalamic pioneer axons fail to form in *Gsx2^{Cre} Pax6* cKOs producing abnormal TCA fasciculation but no changes in topography

The prethalamus has been proposed to host a population of neurons that extend axons to the thalamus which act as "pioneer guides" for TCA navigation (Price et al., 2012; Tuttle et al., 1999). We assessed whether this population is disrupted by Pax6 loss from the prethalamus since, if it is, this might provide an explanation for phenotypes described above.

From about E9.5 on, most cells in the prethalamus express, or are derived from cells that expressed, *Gsx2*. We used a *Gsx2^{Cre}* line (Kessaris et al., 2006) carrying an EGFP Cre reporter (Sousa et al., 2009) to visualize neurons and axons belonging to the *Gsx2* lineage and we observed that prethalamic Pax6-expressing cells are included within the location of the *Gsx2* lineage prethalamic population (Fig. 3A,B). *Zic4* is also expressed by some prethalamic cells, with an onset of expression similar to that of *Gsx2* (about E9.5; Gaston-massuet et al., 2005), and most diencephalic *Zic4* lineage cells express and require Pax6 for their normal development (Li et al., 2018). Using a *Zic4^{Cre}* line (Rubin et al., 2011) we observed that prethalamic neurons derived from *Zic4* lineage were located in a narrow band close to the thalamic-prethalamic border (Fig. 3C-D). We assessed whether these prethalamic populations normally send axons to the thalamus.

Gsx2-lineage GFP-positive axons extended throughout the thalamus forming ordered and parallel projections (Fig. 3E) and running in close apposition to L1-positive TCAs (Fig. 3E',E") from E12.5 onwards (Fig. S2). By contrast, *Zic4*-lineage prethalamic cells did not project axons to the thalamus (Fig. 3D), indicating that

prethalamic pioneer axons arise from *Gsx2*-lineage and not from *Zic4*-lineage prethalamic cells.

Since *Gsx2* is also expressed in the ventral telencephalon (Fig. 3A), and ventral telencephalic neurons are known to project to the thalamus (López-Bendito and Molnár, 2003; Métin and Godement, 1996; Molnár et al., 1998), there was a possibility that *Gsx2*^{Cre} lineage axons innervating the thalamus actually originated from ventral telencephalic neurons. To confirm the existence of *Gsx2*-lineage prethalamic neurons projecting to the thalamus we injected the neuronal tracer Neurobiotin^{TM} in the thalamus of E13.5 *Gsx2*^{Cre} embryos and successfully labelled prethalamic neurons (arrow in Fig. 3F). Neurobiotin^{TM}-positive cells were GFP-expressing *Gsx2* lineage (Fig. 3F-F'',G) and most of them also expressed Pax6 (arrows in Fig. 3H,H'; see summary in Fig. 3I). (Note that individual injections each involved only subregions of the thalamus, explaining why each one only labelled a discrete subset of the prethalamic neurons projecting to the thalamus). This experiment confirmed that *Gsx2*-lineage cells in the prethalamus project to the thalamus.

Having established that pioneer prethalamic axons belong to the *Gsx2* lineage and express Pax6 we next aimed at disrupting their formation by conditionally deleting Pax6 in *Gsx2*-lineage cells. We crossed mice carrying the floxed *Pax6* allele and EGFP Cre reporter with the *Gsx2*^{Cre} line. Pax6 conditional deletion in *Gsx2*-lineage cells (*Gsx2*^{Cre} *Pax6* cKOs) caused a visible reduction in the number of GFP-positive axons projecting from prethalamus to thalamus in E12.5, E13.5 and E14.5 embryos (Fig. 4A-F). These phenotypes were seen consistently in three independent replicates of each genotype at each age. To confirm that the prethalamic axons that were lost in *Gsx2*^{Cre}; *Pax6*$^{loxP/loxP}$ embryos were Pax6-expressing, we used the

DTy54 YAC reporter allele to express tauGFP in cells in which the *Pax6* gene is active, irrespective of whether it is mutant or not (Tyas et al., 2006). Whereas there were many tauGFP-labelled axons running from prethalamus to thalamus in controls, there were very few in experimental embryos (Fig. 4G-J).

DiI placed in the thalamus of E13.5 CAG^{CreER} controls (CAG^{CreER} $Pax6^{fl/+}$; n=3) retrogradely labelled a prethalamic population (arrow in Fig. 4K). In the absence of *Pax6* (CAG^{CreER} *Pax6* cKOs, n=3), no prethalamic cell bodies were labelled by thalamic DiI injection (Fig. 4L), providing further evidence that the prethalamic pioneer population does not form correctly when Pax6 is deleted. Overall, our results show that prethalamic pioneer axons originating from *Gsx2*-lineage cells both express and require Pax6 to develop normal connections with the thalamus (Fig. 4T).

We then studied the TCAs of $Gsx2^{Cre}$ *Pax6* cKOs. Similar to the phenotype described in CAG^{CreER} *Pax6* cKOs, Pax6 deletion in *Gsx2* lineage caused abnormal premature fasciculation of axons crossing the thalamic-prethalamic border, as evidenced by L1 immunohistochemistry (Fig. 4M-R). However, unlike CAG^{CreER} *Pax6* cKOs, $Gsx2^{Cre}$ *Pax6* cKOs did not show abnormal topographical projections, with no obvious overlap between thalamic retrogradely-labelled populations after cortical DiA and DiI placement in caudal and more rostral cortex respectively (Fig. 1B; Fig. 4S) (n=4).

We conclude that, while prethalamic pioneer axons play a role in avoiding premature TCA fasciculation, they are not required for the establishment of accurate thalamocortical topographic mapping (Fig. 4T).

Evidence for the importance of navigational cues in the thalamus itself

We next considered the potential importance of thalamic factors in the establishment of thalamocortical topographic order. Our results above indicate that thalamic axons might have deviated from their normal trajectories before they exited the thalamus in *CAG*^{CreER} *Pax6* cKOs (arrows mark deviant axons in Fig. 1 H',I' and Fig. 1H''; no such axons were observed in the controls, Fig. 1C',E',F'). A misrouting of TCAs in the thalamus was also evident with L1 staining (Fig. 5 A,B). In controls, L1-positive axons showed a high degree of order, forming small, parallel bundles as they exit the thalamus (Fig. 5A), while in *CAG*^{CreER} *Pax6* cKOs they were disorganized. The largest collections of deviant axons were observed projecting from lateral to medial thalamic regions (arrow in Fig. 5B), suggesting that the loss of Pax6 had disrupted normal navigational mechanisms operating within the thalamus.

We looked for evidence that thalamic axons are actively guided through the normal thalamus by using *in vitro* slice culture transplants to assess the effects of repositioning lateral or medial thalamic neurons on the routes taken by their axons. We grafted thalamic slice explants from E13.5 GFP-positive donor embryos into GFP-negative host slices and cultured them for 72 hours to allow thalamic axons to regrow and navigate through the host environment. The donor grafts were positioned so that their axons had to traverse at least 200µm of host thalamic tissue before encountering the Th-PTh boundary, allowing us to assess how the host thalamic tissue affected the trajectory of the axons emerging from the donor tissue. We isolated donor explants from either lateral or medial thalamus, and grafted them either medially or laterally into host thalamus (Fig. 5C,E,G,I).

We found that axons from lateral thalamic explants showed a strong preference to follow a lateral trajectory, irrespective of whether they were grafted laterally or medially (3/3 independent experiments) (Fig. 5C-F). When the lateral axons were

confronted with medial host thalamus, most made a sharp turn towards lateral positions before heading towards the prethalamus (Fig. 5E,F).

When medial explants were grafted into the medial thalamus (Fig. 5G,H), most of them navigated through a medial corridor close to and parallel with the ventricular surface (empty arrow in Fig. 5H), whereas when medial explants were grafted laterally many of their axons turned medially (arrows in Fig. 5J) (5/5 independent experiments). In addition, all transplants of medial grafts, irrespective of their location in the host, generated significant numbers of axons that navigated laterally through the thalamus (Fig. 5H,J).

These results indicated that different subsets of thalamic axons exhibit different chemotactic responses to the thalamic environment and therefore that thalamic axons are actively guided by mechanisms operating within the thalamus itself. To gain further insight into what these mechanisms might be, we went on to examine the expression of guidance molecules in the normal thalamus and in thalamus from which Pax6 has been removed.

Axon guidance molecule expression in normal and Pax6 deficient thalamus

Semaphorin 3a (Sema3a) and Netrin 1 (Ntn1) are secreted guidance molecules whose complementary gradients of expression in the ventral telencephalon are key for the correct establishment of topographical connections between thalamus and cortex (Bielle et al., 2011; Braisted et al., 1999; Molnár et al., 2012; Powell et al., 2008; Wright et al., 2007). Interestingly, we found that their transcripts are also distributed in opposing gradients in the thalamus (Fig. S3A,B). *Ntn1* is most highly expressed at rostral-medial levels (Fig. S3A) while *Sema3a* is most highly expressed in a more caudal-lateral aspect of the thalamus and in the lateral prethalamus (Fig.

S3B). In transverse *in situ* hybridization (ISH) of E13.5 controls we observed that *Ntn1* is expressed in a narrow rostral-medial thalamic population of neurons (arrow in Fig. 6A) while *Sema3a* is expressed in caudal-lateral thalamic neurons (arrows in Fig. 6B) as well as flanking the TCA bundles in the prethalamus (empty arrow in Fig. 6B).

To obtain a clearer three-dimensional view of these expression patterns we reconstructed them from serial, adjacent sections stained for *Sema3a*, *Ntn1*, Pax6 and L1 in controls (Fig. 6C). The scaffold of the 3D model was built from transverse slices stained for DAPI (for the general tissue profile), Pax6 (to define thalamus and prethalamus boundaries) and L1 (to label TCAs). The location of the signalling cues was incorporated within the boundaries of the model by comparing adjacent transverse sections stained for *Sema3a* and *Ntn1*, with dots representing staining density. The 3D reconstruction confirmed that *Sema3a* and *Ntn1* form opposing gradients in the normal embryonic thalamus (Fig. 6C), with *Sema3a* highest at caudal-lateral thalamic levels while *Ntn1* is highest at rostral-medial thalamic levels.

We next investigated the expression patterns of the main receptors for *Ntn1* and *Sema3a* in the thalamus of control embryos. The most interesting finding was that *Unc5c*, encoding a Ntn1 receptor mediating axonal repulsion (Leonardo et al., 1997), was expressed differentially from lateral to medial across the thalamus (Fig. 6D). Laterally, almost all cells expressed high levels of *Unc5c* whereas medially many cells did not (Fig. 6D'). *Unc5c* was largely absent from a narrow strip of cells close to and parallel with the ventricular zone. This strip coincided with the region that contained *Ntn1*-positive cells (compare Fig. 6D and A). *Plxna1*, encoding a Sema3a receptor that mediates repulsion (Rohm et al., 2000; Takahashi et al., 1999;

Tamagnone et al., 1999) was found to be distributed relatively homogenously across the thalamus (Fig. 6E, S3C).

These expression patterns suggest that, whereas all thalamic axons might be repelled by Sema3a (due to their expression of *Plxna1*), only some axons might be repelled by Ntn1 (i.e. those originating laterally, which express *Unc5c*, and those *Unc5c*-expressing axons that originate medially) (Fig. 6K). This could explain why, in the grafting experiments described above, axons from lateral explants invariably navigated laterally, which would be away from medially located high levels of Ntn1. It could also explain why medial explants generated axons able to navigate on a broader front: some axons (those that express *Unc5c*) would be pushed relatively laterally by repulsion from medially expressed *Ntn1*; others (those that do not express *Unc5c*) would be able to maintain a medial trajectory through *Ntn1*-expressing territory, thereby avoiding the high levels of *Sema3a* expressed in lateral thalamus (Fig. 6K).

Other receptor-coding genes analysed (*Dcc*, *Unc5a*, *Unc5d*) showed little or no expression within the main body of the thalamus and are therefore unlikely to contribute to the navigation of thalamic axons within the thalamus (Fig. S3E,G,I).

We next asked whether the thalamic expression of *Ntn1* and *Sema3a* and their receptors change in a way that might explain the medially-directed deviation of lateral axons that we observed in the thalamus of *CAG*^{CreER} *Pax6* cKOs. In these embryos, we found that the medial domain of *Ntn1*-expression was retained and appeared enlarged. *Sema3a* was still expressed higher laterally, although overall levels seemed reduced (Fig. 6F,G). These patterns are reconstructed in 3D in Fig.

6H. *Ntn1* and *Sema3a* expression in the subpallium of *CAG*^{CreER} *Pax6* cKOs appeared to be unaffected (Fig. S3J-M).

Regarding the expression of guidance receptors, fewer laterally-located neurons expressed *Unc5c* in *CAG*^{CreER} *Pax6* cKOs than in controls (compare Fig. 6I' and D'). Significant numbers of *Unc5c*-negative neurons were now intermingled with *Unc5c*-positive neurons even in the most lateral thalamic tissue (Fig. 6I'). *Plxna1*'s thalamic expression pattern did not change in the absence of Pax6 (Fig. 6J, S3D), nor did that of any of the other receptor-coding genes studied (Fig. S3E-J).

As reported above, we discovered that *CAG*^{CreER} *Pax6* cKOs show a misrouting in a medial direction of axons from the lateral thalamus (Fig. 1), and our finding that many laterally-located thalamic neurons lose their expression of *Unc5c*, provides a likely explanation, summarized in Fig. 6L. We propose that *Unc5c*-negative laterally-located thalamic neurons in *CAG*^{CreER} *Pax6* cKO thalamus would no longer be repelled from the medial thalamus by its high levels of *Ntn1*. Consequently, they would be more likely to stray, or perhaps to be pushed by relatively high lateral levels of *Sema3a*, towards a medial direction (Fig. 6L). Overall, our findings indicate that mechanisms exist within the thalamus itself to ensure that its TCAs exit in an orderly manner and that these mechanisms play an important part in the correct topographic mapping of TCAs onto the cortex.

DISCUSSION

During embryonic development, thalamic axons undertake a long journey, having to navigate through several tissues before they arrive to the cortex. It is therefore crucial that their guidance is tightly regulated by mechanisms placed all along the route. Previous studies have demonstrated the importance of the ventral

telencephalon as an intermediate target for the establishment of correct topographical connections between thalamus and cortex. Here, gradients of signalling molecules seem to sort different subsets of TCAs towards different areas of the embryonic cortex (Antón-Bolaños et al., 2018; Bielle et al., 2011; Braisted et al., 1999; Dufour et al., 2003; Métin and Godement, 1996; Molnár et al., 2012; Vanderhaeghen and Polleux, 2004). To date, the importance of other tissues along the route in the establishment and/or maintenance of axonal topography remained unexplored. In this work, we show that if thalamic axons do not emerge in order from the thalamus they will connect with the wrong areas of the cortex, resulting in topographical defects of the thalamocortical tract. This highlights the importance of maintaining axonal order throughout the route and suggests the existence of guidance mechanisms within the diencephalon to guarantee this happens.

Indeed, our *in vitro* graft experiments demonstrated that the embryonic thalamic tissue is instructive for TCAs and seems to sort axons according to their original medio-lateral position. We went on to find a possible guidance mechanism acting within the thalamus. The thalamus expresses *Ntn1* and *Sema3a,* some of the same guidance molecules known to guide TCAs in the ventral telencephalon (Bielle et al., 2011; Powell et al., 2008; Wright et al., 2007). What is more, there is an interesting correspondence between the regions expressing each of those molecules in the thalamus and in the ventral telencephalon. TCAs that emerge and navigate through the *Sema3a*-high region of the thalamus (lateral-caudal thalamus, dLGN) are steered towards the *Sema3a*-high region in the ventral telencephalon, while axons that emerge and navigate through the *Ntn1*-high region of the thalamus (ventral-medial thalamus,VMP) are sorted towards *Ntn1*-high regions in the ventral telencephalon. This suggests that each subset of thalamic axons might maintain the expression of

399 the same combination of axon guidance receptors along the route and therefore
400 show the same chemotactic response when confronting gradients of signalling cues.
401 Likewise, it indicates that the same gradients of guidance molecules are re-used at
402 different levels of the thalamocortical pathway to maintain topographic order.

403 The chemotactic behaviour of TCAs with respect to *Sema3a* and *Ntn1* gradients in
404 the thalamus and ventral telencephalon can be explained by our observations of the
405 expression of Sema3a and Ntn1 receptors in developing thalamus. We show that all
406 thalamic neurons seem to express homogeneous levels of *Plxna1*, a receptor
407 mediating repulsion to Sema3a (Rohm et al., 2000; Takahashi et al., 1999;
408 Tamagnone et al., 1999), while Unc5c, a receptor mediating repulsion to Ntn1
409 (Leonardo et al., 1997), was found to be expressed in a lateral-high medial-low
410 gradient. According to these observations, we propose a model in which
411 complementary expression patterns of Sema3a and Ntn1 can establish
412 topographical order on TCAs by a mechanism of double repulsion, in which all
413 thalamic axons have the potential to be repelled by Sema3a but only lateral axons
414 are additionally repelled by Ntn1. It is possible that laterally-derived axons
415 experience stronger Ntn1 repulsion the more lateral they are. Thus, lateral thalamic
416 axons prefer to navigate through Sema3a-high, Ntn1-low regions because they
417 might be more strongly repelled by Ntn1 than by Sema3a. Axons located in
418 intermediate regions of the thalamus express lower levels of Unc5c, thus they might
419 be equally repelled by Sema3a and Ntn1 and chose to navigate across regions with
420 moderate levels of both signalling cues. Likewise, medial axons are only repelled by
421 Sema3a and neutral to Ntn1, therefore they chose to navigate through Sema3a-low,
422 Ntn1-high areas.

Supporting this model are the experiments showing that TCAs are repelled by Nnt1 (Bielle et al., 2011; Bonnin et al., 2007; Powell et al., 2008) and thalamic growth cones show retraction behaviour in the presence of Sema3a (Bagnard et al., 2001). Moreover, Wright and colleagues reported that in mice harbouring a mutation that makes the axons non responsive to Sema3a, axons from the ventrobasal (VB) thalamic nucleus, were caudally shifted and target the visual cortex instead of the somatosensory cortex (Wright et al., 2007). Our double repulsion model satisfactorily explains this phenotype. The VB nucleus is located in an intermediate thalamic region that would contain substantial number of Unc5c-positive neurons. In those mutants, VB axons lose their repulsion to Sema3a but many would still be repelled by Ntn1, and therefore would steer towards Sema3a-high, Ntn1-low regions both in the thalamus and the ventral telencephalon.

The behaviour of the TCAs in our explant experiments also supports the double repulsion model. Explants from lateral thalamus, which express high levels of Unc5c, invariably navigate through lateral areas of the thalamus, away from the Ntn1-rich area in the medial thalamus. Explants from medial thalamus show a preference to navigate through a medial corridor, parallel to the ventricular surface, where levels of Ntn1 are higher. These TCAs probably correspond with the subset of neurons in the medial thalamus that do not express Unc5c, and therefore are repelled by Sema3a but neutral to Ntn1. Medial explants also produce axons exhibiting a mixture of trajectories towards more lateral thalamic areas. This is compatible with the fact that a subset of medial thalamic neurons express variable levels of Unc5c, and thus are repelled with variable strength from the medial thalamus. Finally, in Pax6 deficient embryos, many lateral thalamic neurons downregulate Unc5c, while the levels of Plxna1 seem unaffected, meaning that lateral TCAs lose their repulsion to Ntn1 but

448 they are still repelled by lateral Sema3a. This might explain why in these mutants,
449 lateral thalamic axons are misrouted towards medial thalamic regions and
450 subsequently take the pathway medial thalamic axons normally do.

451 Other molecules known to form gradients and guide TCAs in the ventral
452 telencephalon, like Slit1 or Ephrin A5 (Bielle et al., 2011; Dufour et al., 2003; Molnár
453 et al., 2012; Seibt et al., 2003; Vanderhaeghen and Polleux, 2004) were not
454 analysed in this study. It remains to be tested whether these molecules and their
455 receptors are also expressed in the thalamus in a gradient fashion and if they follow
456 the same rules proposed in our model.

457 It is important to highlight that in this study we only considered the medio-lateral axis
458 of the main thalamic body, but the same or other guidance cues and receptors
459 probably function in other directions. For example, work in mice showed that Unc5c
460 (Bonnin et al., 2007) and DCC (Powel et al., 2008) are also highly expressed in the
461 rostral thalamus, at a level we did not cover in our expression and tracer analyses.
462 Therefore, other axes of the thalamus important for the establishment of
463 thalamocortical topography remain to be explored.

464 Another important question is why thalamic axons exit the thalamus at all. Why do
465 they navigate towards the prethalamus and not in another direction, for example
466 towards the pretectum? One previously suggested mechanism was that TCAs follow
467 the path pioneered by axons that develop in the opposite direction from prethalamus
468 to thalamus (Braisted et al., 1999; Mitrofanis and Guillery, 1993; Molnár et al., 1998;
469 Qin et al., 2019). In this work, we disrupted the formation of these pioneer axons and
470 found that TCAs not only are able to exit the thalamus but they also reach the cortex
471 and establish correct topographic connections. Therefore, there must be other

mechanisms in place to direct TCAs out of the thalamus. Our 3D reconstruction revealed that, besides the medio-lateral Sema3a gradient, this guidance cue is also higher posteriorly, where the thalamus meets the pretectum and lower anteriorly, close to the prethalamus. According to our model, all TCAs are equally repelled by Sema3a, therefore this directionality of the Sema3a gradient could serve to repel all TCAs out of the thalamus.

Finally, our results have given some interesting new insights into the development and the importance of the pioneer axons from the prethalamus to the thalamus. First, we found that the prethalamic neurons extending pioneer axons to the thalamus belong to a particular lineage, the Gsx2-lineage and not the Zic4-lineage. Second, although disturbing the prethalamus-to-thalamus pioneers did not stop TCAs reaching the cortex without any topographic error, it did cause them to fasciculate prematurely as they crossed the prethalamus. Growing axons often increase their fasciculation when they cross regions that are hostile to their growth. Our and other studies have shown that the prethalamus also expresses guidance cues with potential to exert a repulsive response of TCAs (Ono et al., 2014), thus it is possible that interactions between the developing TCAs and prethalamic pioneers somehow helps the passage of the TCAs across this region. Further work is needed to discover what the consequences are if this help is unavailable.

Material and Methods

Mice

All animals (*Mus musculus*) were bred according to the guidelines of the UK Animals (Scientific Procedures) Act 1986 and all procedures were approved by Edinburgh University's Animal Ethics Committee.

For conditional inactivation of Pax6, we used a tamoxifen-inducible $Pax6^{loxP}$ allele (Simpson et al., 2009) and a RCE:LoxP EGFP Cre reporter allele (Sousa et al., 2009) and we combined them with different Cre lines. To generate a deletion of Pax6 throughout the embryo, we used lines carrying a CAGGCre-ER^{TM} allele (Hayashi and McMahon, 2002; Quintana-Urzainqui et al., 2018). To inactivate Pax6 in different parts of the prethalamus we used either a Gsx2-Cre (Kessaris et al., 2006) or the Zic4-Cre allele (Rubin et al., 2011). For cortex-specific deletion of Pax6, we used Emx1Cre-ER^{T2} (Kessaris et al., 2006).

The DTy54 YAC reporter allele (Tyas et al., 2006) was combined with the Gsx2-Cre allele to generate Gsx2Cre; $Pax6^{loxP/loxP}$ embryos expressing tauGFP in cells in which the Pax6 gene is active.

Embryos heterozygous for the $Pax6^{loxP}$ allele ($Pax6^{fl/+}$) were used as controls since previous studies have shown no detectable defects in the forebrain of $Pax6^{fl/+}$ embryos (Simpson et al., 2009). Embryos carrying two copies of the floxed Pax6 allele ($Pax6^{fl/fl}$) were the experimental conditional knock-out (cKO) groups.

For thalamic explant experiments, we generated litters containing GFP-positive and negative embryos by crossing a line of heterozygous studs for a constitutively active

form of CAGGCre-ER^{TM} allele and the and a RCE:LoxP EGFP Cre reporter allele with wild type females.

The day the vaginal plug was detected was considered E0.5. Pregnant mice were given 10mg of tamoxifen (Sigma) by oral gavage on embryonic day 9.5 (E9.5) and embryos were collected on E12.5, E13.5, E14.5, E15.5, E16.5 or E18.5 For the DiI and DiA tracing experiments, wild type embryos (CD1 background) were additionally used as controls.

Immunohistochemistry

Embryos were decapitated and fixed in 4% paraformaldehyde (PFA) in phosphate buffered saline (PBS) overnight at 4^{o}C. After washes in PBS, heads were cryoprotected by immersion in 30% sucrose in PBS, embedded in OCT Compound and sectioned using a cryostat at 10µm.

Cryo-sections were let to stabilize at room temperature for at least 2 hours and then washed three times in PBST (1X PBS with 0.1% Triton X-100, Sigma). To block endogenous peroxidase, sections were treated with 3% H_2O_2 for 10 minutes. After PBS washes, antigen retrieval was performed by immersing the sections in Sodium Citrate buffer (10mM, pH6) heated at approximate 90°C using a microwave for 20 minutes. Sections were then incubated with the rabbit polyclonal anti-Pax6 (1:200, BioLegend Cat # 901302) overnight at 4°C. The secondary antibody (goat anti-rabbit bioninylated, 1:200, Vector laboratories Cat # BA-1000) was incubated for 1 hour at room temperature followed by a 30-minute incubation with Avidin-Biotin complex (ABC kit, Vector laboratories Cat # PK6100). Finally, diaminobenzidene (DAB, Vector Laboratories, Cat # SK4100) reaction was used to obtain a brown precipitate and sections were mounted in DPX media (Sigma-Aldrich, Cat # 06522).

For immunofluorescence, cryosections were incubated overnight at 4°C with the following primary antibodies: rat monoclonal anti-Neural Cell Adhesion Molecule L1 (1:500 Millipore, Cat # MAB5272, clone 324), rabbit polyclonal anti-Pax6 (1:200, BioLegend Cat # 901302), goat polyclonal anti-GFP (1:200, Abcam Cat # ab6673), rabbit polyclonal anti-GFP (1:200, Abcam Cat # ab290). The following secondary antibodies from Thermo Fisher Scientific were incubated at room temperature for one hour: Donkey anti-rat Alexa^{488} (1:100, Thermo Fisher, Cat # A-21208), Donkey anti-rat Alexa^{594} (1:100, Thermo Fisher, Cat # A-21209), Donkey anti-rabbit Alexa^{568} (1:100, Thermo Fisher, A10042), Donkey anti-rabbit Alexa^{488} (1:100, Thermo Fisher Cat # R37118), Donkey anti-goat Alexa^{488} (1:100, Invitrogen, Cat # A11055). Sections were counterstained with DAPI (Thermo Fisher Scientific, Cat # D1306) and mounted in ProLong Gold Antifade Mountant (Thermo Fisher Scientific, Cat # P36930).

In situ **hybridization**

In vitro transcription of digoxigenin-labelled probes was done with DIG RNA-labeling kit (Sigma-Aldrich, Cat # 11175025910). The following digoxigenin-labelled probes were synthetized in the lab from cDNA: Ntn1 (kindly donated by Dr Thomas Theil; forward primer: CTTCCTCACCGACCTCAATAAC, reverse primer: GCGATTTAGGTGACACTATAGTTGTGCC TACAGTCACACACC), Sema3a (forward primer: ACTGCTCTGACTTGGAGGAC, reverse primer: ACAAACACGAGTGCTGGTAG), Plxna1 (forward primer: GACGAGATTCTGGTGGCTCT, reverse primer: CATGGCAGGGAGAGGAAGG), DCC (forward primer: AACAGAAGGTCAAGCACGTG, reverse primer: CAATCACCACGACCAACACA), Unc5a (forward primer: CTGTCAGACCCTGCTGAGT, reverse primer: GGGCTAGAGTTCGCCAGTC),

562 Unc5d (forward primer: GGACAGAGCTGAGGACAACT, reverse primer:
563 GTATCAAACGTGGCGCAGAT). Unc5c probe was kindly donated by Dr. Vassiliki
564 Fotaki, University of Edinburgh, UK and Dr Suran Ackerman, UCSanDiego, USA).
565 Cryosections were processed for *in situ* hybridization (ISH) using standard protocols.
566 Some slides were counterstained for nuclear fast red (Vector Laboratories, Cat# LS-
567 J1044-500).

568 **Axon Tract Tracing**

569 For cortical injections, brains were dissected between E15.5 and E18.5 and fixed in
570 4% PFA in PBS at 4^{o}C for at least 48 hours. After washes in PBS, filter paper
571 impregnated in DiI (NeuroVue Red, Molecular Targeting Technologies, Cat # FS-
572 1002) and DiA (NeuroVue Jade, molecular Targeting Technologies, Cat # FS-1006)
573 was inserted approximately in the somatosensory and visual areas of the cortex,
574 respectively. Brains were incubated at 37^{o}C in PBS for 4 weeks to allow the diffusion
575 of the tracers.

576 For thalamic injections in fixed tissue, embryos were dissected at E13.5 and fixed
577 overnight in 4%PFA in PBS at 4^{o}C. After PBS washes, brains were cut in half at the
578 midline and DiI was inserted in the thalamus using a fine probe. Brains were
579 incubated for 1 week in PBS at 37^{o}C.

580 Brains were then cryoprotected in 30% sucrose, embedded in OCT Compound and
581 sectioned in a cryostat at 30µm. Sections were counterstained with DAPI diluted
582 1:1000 in distilled water.

583 For thalamic injections in non-fixed tissue, we applied neurobiotin (Vector
584 Laboratories, Cat # SP-1120), and amino derivative of biotin used as an intracellular
585 label for neurons. The tracer in powder was held at the tip of an entomological

needle (00) and recrystallized using vapour from distilled water. Brains were cut in half and the crystal was inserted in the thalamus. Brains were then immersed in continuously oxygenated Ringer (124mM NaCl, 5mM KCl, 1.2mM KH_2P0_4, 1.3mM $MgSO_4$ $7H_2O$, 26mM $NaHCO_3$, 2.4mM $CaCl_2$ $2H_2O$, 10mM glucose) and incubated overnight at RT.The tissue was fixed in 4% PFA in PBS overnight at 4°C, washed in PBS, cryoprotected in 30% sucrose and sectioned in a cryostat at 10µm. Neurobiotin was visualized by incubating the sections with either $Strep^{488}$ or $Strep^{546}$.

Thalamic explants and slice culture

E13.5 embryos were dissected, embedded in 4% low melting temperature agarose (Lonza, Cat # 50100) and sectioned in a vibratome to produce 300µm-thick coronal slices. Lateral or medial thalamic explants were dissected from slices belonging to GFP-positive embryos and transplanted into equivalent rostral/caudal slices belonging to GFP-negative embryos (see schemas in Fig. 5). The thalamus and its different medio-lateral regions were recognized under the dissecting scope by anatomical landmarks. Slices were then cultured for 72 hours in floating membranes (Whatman nuclepore track-etched membranes, Cat# WHA110414) over serum-free Neurobasal medium (Thermo Fisher Scientific, Cat# 21103049) in 60mm center well organ culture dishes (Falcon, Cat# 353037). Cultures were fixed in 4% PFA overnight at 4°C, cryoprotected in 30% sucrose and cryosectioned at 10µm to be processed for immunofluorescence.

Quantifications of numbers of axons and bundle width

Images were blinded-analysed for at least three embryos for each condition. We positioned three lines across the prethalamus (as specified in Results) and generated a L1 intensity profile using Fiji Software (Schindelin et al., 2012). Intensity

profiles were then processed by tracing a line at an arbitrary (but constant for all quantifications) intensity level and quantifying the number and width of bundles crossing the line. Statistical significance was assessed applying two-tailed unpaired Student's t-test and N=3.

3D reconstruction

We used Free-D software (Andrey and Maurin, 2005) to reconstruct the structure of thalamus and prethalamus from transverse slices stained with DAPI and antibodies against L1 and Pax6 to reveal the thalamocortical tract and the limits of the diencephalic structures, respectively. The thalamus territory was recognisable by an intense DAPI staining and Pax6-negative mantle zone, contrasting with prethalamus and pretectum, which express high levels of Pax6 in the postmitotic neurons. The location of the signalling molecules was included in the model by comparison of transversal and sagittal sections stained for Ntn1 and Sema3a and their adjacent sections processed for Pax6 and L1 with the sections used to build the model scaffold. Dots are representation of staining density.

Microscopy and imaging

ISH and IHQ images were taken with a Leica DMNB microscope coupled to a Leica DFC480 camera. Fluorescence images were taken using a Leica DM5500B automated epifluorescence microscope connected to a DFC360FX camera. Image panels were created with Adobe Photoshop CS6.

Acknowledgements

We thank Dr Vassiliki Fotaki for providing the Unc5c probe.

Competing interests

No competing interests.

Funding

This work was supported by a Marie Curie Fellowship from the European Commission [624441]; a Medical Research Council UK Research Grant [N012291] and a Biotechnology and Biological Sciences Research Council UK Research Grant [N006542].

References

Amassian, V. and Weiner, H. (1966) Monosynaptic and polysynaptic activation of pyramidal tract neurons by thalamic stimulation. In *The thalamus* (ed. D.P. Purpura and M.D. Yahr editors), pp 255–282. New York: Columbia University Press.

Andrey, P. and Maurin, Y. (2005). Free-D: an integrated environment for three-dimensional reconstruction from serial sections. *J. Neurosci. Methods* **145**, 233–244.

Angevine, J. A. Y. B. (1970). Time of Neuron Origin in the Diencephalon of the Mouse . An Autoradiographic Study '.

Antón-Bolaños, N., Espinosa, A. and López-Bendito, G. (2018). Developmental interactions between thalamus and cortex: a true love reciprocal story. *Curr. Opin. Neurobiol.* **52**, 33-41.

Auladell, C. and Hans, P. P. (2000). The early development of thalamocortical and corticothalamic projections in the mouse. Anat Embryol **201**, 169–179.

Bagnard, D., Chounlamountri, N., Püschel, A.W., Bolz, J. (2001). Axonal Surface Molecules Act in Combination with Semaphorin 3A during the Establishment of Corticothalamic Projections. *Cereb. Cortex* **11**, 278–285.

Bielle, F., Marcos-Mondéjar, P., Leyva-Díaz, E., Lokmane, L., Mire, E., Mailhes, C., Keita, M., García, N., Tessier-Lavigne, M., Garel, S., et al. (2011). Emergent growth cone responses to combinations of Slit1 and Netrin 1 in thalamocortical axon topography. *Curr. Biol.* **21**, 1748–1755.

Bonnin, A., Torii, M., Wang, L., Rakic, P. and Levitt, P. (2007). Serotonin modulates the response of embryonic thalamocortical axons to netrin-1. **10**, 588–597.

Bosch-Bouju, C., Hyland, B. I. and Parr-Brownlie, L. C. (2013). Motor thalamus integration of cortical, cerebellar and basal ganglia information: implications for normal and parkinsonian conditions. *Front. Comput. Neurosci.* **7**, 1–21.

Braisted, J. E., Tuttle, R. and Leary, D. D. M. O. (1999). Thalamocortical Axons Are Influenced by Chemorepellent and Chemoattractant Activities Localized to Decision Points along Their Path. **440**, 430–440.

Caballero, I. M., Manuel, M. N., Molinek, M., Quintana-Urzainqui, I., Mi, D., Shimogori, T. and Price, D. J. (2014). Cell-Autonomous Repression of Shh by Transcription Factor Pax6 Regulates Diencephalic Patterning by Controlling the Central Diencephalic Organizer. *Cell Rep.* **8**, 1405–1418.

Clegg, J. M., Li, Z., Molinek, M., Caballero, I. M., Manuel, M. N. and Price, D. J. (2015). Pax6 is required intrinsically by thalamic progenitors for the normal molecular patterning of thalamic neurons but not the growth and guidance of their axons. *Neural Dev.* 1–12.

Dufour, A., Seibt, J., Passante, L., Depaepe, V., Ciossek, T., Frisén, J., Kullander, K., Flanagan, J. G., Polleux, F. and Vanderhaeghen, P. (2003). Area specificity and topography of thalamocortical projections are controlled by ephrin/Eph genes. *Neuron*

39, 453–465.

Fukuda, T., Kawano, H., Ohyama, K. and Li, H. (1997). of Neurocan and L1 in the Formation of Thalamocortical Pathway. **152**, 141–152.

Gaston-massuet, C., Henderson, D. J., Greene, N. D. E. and Copp, A. J. (2005). Zic4 , a Zinc-finger transcription factor, is expressed in the developing mouse nervous system. **233**, 1110–1115.

Georgala, P. A., Carr, C. B. and Price, D. J. (2011). The role of Pax6 in forebrain development. *Dev. Neurobiol.* **71**, 690–709.

Hayashi, S. and McMahon, A. P. (2002). Efficient Recombination in Diverse Tissues by a Tamoxifen-Inducible Form of Cre: A Tool for Temporally Regulated Gene Activation/Inactivation in the Mouse. *Dev. Biol.* **244**, 305–318.

Jones, L., López-bendito, G., Gruss, P., Stoykova, A. and Molnár, Z. (2002). Pax6 is required for the normal development of the forebrain axonal connections. **5052**, 5041–5052.

Jones, E. G. (2007). The Thalamus. 2nd Edn. Cambridge: Cambridge University Press.

Kessaris, N., Fogarty, M., Iannarelli, P., Grist, M., Wegner, M. and Richardson, W. D. (2006). Competing waves of oligodendrocytes in the forebrain and postnatal elimination of an embryonic lineage. *Nat. Neurosci.* **9**, 173–179.

Leonardo, E. D., Hinck, L., Masu, M., Keino-Masu, K., Ackerman, S. L. and Tessier-Lavigne, M. (1997). Vertebrate homologues of C. elegans UNC-5 are candidate netrin receptors. *Nature* **386**, 833–838.

Li, Z., Pratt, T. and Price, D. J. (2018). Zic4 -Lineage Cells Increase Their Contribution to

Visual Thalamic Nuclei during Murine Embryogenesis If They Are Homozygous or Heterozygous for Loss of Pax6 Function. *eNeuro* **1**, 1–19.

Lopez-Bendito, G., Cautinat, A., Sanchez, J. A., Bielle, F., Flames, N., Garratt, A. N., Talmage, D. A., Role, L. W., Charnay, P., Marin, O., et al. (2006). Tangential neuronal migration controls axon guidance: a role for neuregulin-1 in thalamocortical axon navigation. *Cell* **125**, 127–142.

López-Bendito, G. and Molnár, Z. (2003). Thalamocortical development: How are we going to get there? *Nat. Rev. Neurosci.* **4**, 276–289.

Manuel, M. N., Mi, D., Mason, J. O. and Price, D. J. (2015). Regulation of cerebral cortical neurogenesis by the Pax6 transcription factor. *Front. Cell. Neurosci.* **9**, 1–21.

Métin, C. and Godement, P. (1996). The Ganglionic Eminence May Be an Intermediate Target for Corticofugal and Thalamocortical Axons. *J. Neurosci.* **16**, 3219–3235.

Mi, D., Carr, C. B., Georgala, P. A., Huang, Y. T., Manuel, M. N., Jeanes, E., Niisato, E., Sansom, S. N., Livesey, F. J., Theil, T., et al. (2013). Pax6 Exerts regional control of cortical progenitor proliferation via direct repression of Cdk6 and Hypophosphorylation of pRb. *Neuron* **78**, 269–284.

Mitrofanis, J. and Guillery, R. W. (1993). New views of the thalamic reticular nucleus in the adult and the developing brain. *Trends Neurosci.*

Molnár, Z., Adams, R. and Blakemore, C. (1998). Mechanisms Underlying the Early Establishment of Thalamocortical Connections in the Rat. *J. Neurosci.* **18**, 5723–5745.

Molnár, Z., Garel, S., López-bendito, G., Maness, P. and Price, J. (2012). Mechanisms Controlling the Guidance of Thalamocortical Axons Through the Embryonic Forebrain.

35, 1573–1585.

Ohyama, K., Tan-takeuchi, K., Kutsche, M., Schachner, M., Uyemura, K. and Kawamura, K. (2004). Neural cell adhesion molecule L1 is required for fasciculation and routing of thalamocortical fibres and corticothalamic fibres. **48**, 471–475.

Ono, K., Clavairoly, A., Nomura, T., Gotoh, H., Uno, A., Armant, O., Takebayashi, H., Zhang, Q., Shimamura, K., Itohara, S., et al. (2014). Development of the prethalamus is crucial for thalamocortical projection formation and is regulated by Olig2. **5**, 2075–2084.

Parish, E. V., Mason, J. O. and Price, D. J. (2016). Expression of Barhl2 and its relationship with Pax6 expression in the forebrain of the mouse embryo. *BMC Neurosci.* **17**, 1–16.

Piñon, M. C., Tuoc, T. C., Ashery-padan, R. and Stoykova, A. (2008). Altered Molecular Regionalization and Normal Thalamocortical Connections in Cortex-Specific Pax6 Knock-Out Mice. **28**, 8724–8734.

Powell, A. W., Sassa, T., Wu, Y., Tessier-lavigne, M. and Polleux, F. (2008). Topography of Thalamic Projections Requires Attractive and Repulsive Functions of Netrin-1 in the Ventral Telencephalon. **6**, e116.

Pratt, T., Vitalis, T., Warren, N., Edgar, J. M., Mason, J. O. and Price, D. J. (2000). A role for Pax6 in the normal development of dorsal thalamus and its cortical connections. *Development* **127**, 5167-5178.

Price, D. J., Clegg, J., Duocastella, X. O., Willshaw, D. and Pratt, T. (2012). The importance of combinatorial gene expression in early mammalian thalamic patterning and thalamocortical axonal guidance. **6**, 1–15.

Qin, J., Wang, M., Zhao, T., Xiao, X., Li, X., Yang, J., Yi, L., Goffinet, A. M., Qu, Y. and Zhou,

L. (2019). Early Forebrain Neurons and Scaffold Fibers in Human Embryos. *Cereb. Cortex* 1–16.

Quintana-Urzainqui, I., Kozic, Z., Tian, T., Manuel, M., Mason, J. O., Price, D. J., Mitra, S., Tian, T., Manuel, M. and Mason, J. O. (2018). Tissue-Specific Actions of Pax6 on Proliferation and Differentiation Balance in Developing Forebrain Are Foxg1 Dependent. **10**, 171–191.

Rohm, B., Ottemeyer, A., Lohrum, M. and Puschel, A. W. (2000). Plexin/neuropilin complexes mediate repulsion by the axonal guidance signal semaphorin 3A. *Mech. Dev.* **93**, 95–104.

Rubin, A. N., Alfonsi, F., Humphreys, M. P., Choi, C. K. P. and Susana, F. (2011). The germinal zones of the basal ganglia but not the septum generate GABAergic interneurons for the cortex. **30**, 12050–12062.

Schindelin, J., Arganda-Carreras, I., Frise, E., Kaynig, V., Longair, M., Pietzsch, T., Preibisch, S., Rueden, C., Saalfeld, S., Schmid, B., et al. (2012). Fiji: an open-source platform for biological-image analysis. *Nat. Methods* **9**, 676–682.

Seibt, J., Schuurmans, C., Dehay, C., Vanderhaeghen, P., Hill, C. and Carolina, N. (2003). Neurogenin2 Specifies the Connectivity of Thalamic Neurons by Controlling Axon Responsiveness to Intermediate Target Cues. **39**, 439–452.

Simpson, T. I., Pratt, T., Mason, J. O. and Price, D. J. (2009). Normal ventral telencephalic expression of Pax6 is required for normal development of thalamocortical axons in embryonic mice. **5**, 1–18.

Sousa, V. H., Miyoshi, G., Hjerling-Leffler, J., Karayannis, T. and Fishell, G. (2009).

764 Characterization of Nkx6-2-derived neocortical interneuron lineages. *Cereb. Cortex* **19**.

765 **Stoykova, A., Fritsch, R., Walther, C. and Gruss, P.** (1996). Forebrain patterning defects in
766 Small eye mutant mice. *Development* **122**, 3453-3465.

767 **Takahashi, T., Fournier, A., Nakamura, F., Wang, L. H., Murakami, Y., Kalb, R. G., Fujisawa,**
768 **H. and Strittmatter, S. M.** (1999). Plexin-neuropilin-1 complexes form functional
769 semaphorin-3A receptors. *Cell* **99**, 59–69.

770 **Tamagnone, L., Artigiani, S., Chen, H., He, Z., Ming, G. I., Song, H., Chedotal, A., Winberg,**
771 **M. L., Goodman, C. S., Poo, M., et al.** (1999). Plexins are a large family of receptors for
772 transmembrane, secreted, and GPI-anchored semaphorins in vertebrates. *Cell* **99**, 71–
773 80.

774 **Tlamsa, A. P. and Brumberg, J. C.** (2010). Organization and morphology of thalamocortical
775 neurons of mouse ventral lateral thalamus. *Somatosens. Mot. Res.* **27**, 34–43.

776 **Tuttle, R., Nakagawa, Y., Johnson, J. E. and Leary, D. D. M. O.** (1999). Defects in
777 thalamocortical axon pathfinding correlate with altered cell domains in Mash-1-
778 deficient mice. **1916**, 1903–1916.

779 **Tyas, D. A., Simpson, T. I., Carr, C. B., Kleinjan, D. A., van Heyningen, V., Mason, J. O. and**
780 **Price, D. J.** (2006). Functional conservation of Pax6 regulatory elements in humans and
781 mice demonstrated with a novel transgenic reporter mouse. *BMC Dev. Biol.* **6**, 1–11.

782 **Vanderhaeghen, P. and Polleux, F.** (2004). Developmental mechanisms patterning
783 thalamocortical projections: Intrinsic, extrinsic and in between. *Trends Neurosci.* **27**,
784 384–391.

785 **Visel, A., Thaller, C. and Eichele, G.** (2004). GenePaint.org: an atlas of gene expression

patterns in the mouse embryo. *Nucleic Acids Res.* **32**, D552-6.

Walther, C. and Gruss, P. (1991). Pax-6, a murine paired box gene, is expressed in the developing CNS. *Development* **113**, 1435-1449.

Warren, N. and Price, D. J. (1997). Roles of Pax-6 in murine diencephalic development. *Development* **124**, 1573-1582.

Wright, A. G., Demyanenko, G. P., Powell, A., Schachner, M., Enriquez-barreto, L., Tran, T. S., Polleux, F. and Maness, P. F. (2007). Close Homolog of L1 and Neuropilin 1 Mediate Guidance of Thalamocortical Axons at the Ventral Telencephalon. **27**, 13667–13679.

Figure legends

Figure 1. Ubiquitous conditional Pax6 deletion at E9.5 causes mapping errors in the thalamocortical connection. A) Schema showing how thalamic axons map to specific areas of the cortex via the thalamocortical pathway. **B)** Schematic drawing representing the cortical location were the tracers were placed at E15.5. DiA was positioned in the caudal (visual) cortex while DiI was position in more rostral areas (approximately somatosensory cortex). **C-I)** Fluorescent microphotographs showing cells and axons retrogradely labelled by DiI and DiA. While in controls (C-F) the areas labelled in the thalamus were clearly separated (dotted lines), in CAG^{CreER} Pax6 cKOs (G-I) they visibly overlapped, indicating the existence of mapping errors in these mutants. Arrows in G,H and I indicate that the thalamocortical bundle was segregated in visual (green) and somatosensory (red) halves at the level of their exit from the diencephalon. **C',E',F',H',I')** High power images from insets in C,E,F,H and I, respectively, where only the DiI channel is shown. Arrows in H' and I' point to DiI-labeled axons showing abnormal trajectories towards medial thalamic regions. **L)** Schematic summary of the tract tracing results. Scale bars: 200µm (C,D,G); 50µm (C',E',F',H',I'). All phenotypes were observed at least in three independent biological replicates (embryos from three different litters). Ctx= cortex, OB= Olfactory Bulb, Pth= prethalamus, Th= thalamus, vTel= ventral telencephalon, WT= wild type.

Figure 2. Thalamic axons exhibit abnormal fasciculation as they cross the prethalamus in CAG^{CreER} Pax6 cKOs. A-L) Transverse (A,B, F-I) and sagittal (C-D, J-L) sections showing immunofluorescence for L1 and Pax6 in controls (A-E) and CAG^{CreER} Pax6 cKOs (F-L) at E13.5. White arrows in A,B and E show the point at which the thalamocortical tract forms a single bundle and exits the diencephalon in controls. Empty arrows in G-I and L point to thalamic axons converging prematurely

into big bundles as soon as they cross the thalamic-prethalamic boundary in Pax6 cKOs. Discontinuous lines in A, F-I mark the thalamic-prethalamic boundary. Discontinuous lines in B mark the level of sections in C, D and E. Discontinuous lines in D,E,K and L show the position of the lines used to quantify the number and width of bundles crossing the prethalamus. **M,N)** Examples of the measurements taken for the quantifications of the number and width of axon bundles crossing each line. Individual bundles were identified as single L1-positive structure above a consistent intensity threshold (red lines). **O,P)** Graphs showing the quantification of the number (O) and width (P) of axon bundles crossing each reference line and the statistical significance. Representation of means +/- SEM, n=3, where *, ** and *** stand for a p-value ≤ 0.05, 0.01 and 0.001 respectively after two-tailed unpaired Student's t-test and N=3. O) We found a significant decrease in the number of bundles crossing all three checkpoints (Th-PTh boundary: p value=0.046, t=2.86, df=4; Mid Pth: p value=0.0085, t=4.82, df=4; low-PTh: p-value=0.012, t=4.39, df=4). P) We detected a big increase in axon bundle width at the Th-PTh border (p-value<<0.001, t=9.12, df=443) and the mid-PTh (p-value<< 0.001, t=7.21, df=350), but no significant change at the low-PTh. **Q)** Schematic summary of the results showing how thalamic axons undergo abnormal and premature fasciculation when crossing the prethalamus in CAG^{CreER} Pax6 cKOs. Scale bars: 200µm. Ctx= cortex, Pth= prethalamus, TCA=thalamocortical axons, Th= thalamus, vTel= ventral telencephalon.

Figure 3. Prethalamic pioneer axons belong to the Gsx2 lineage and express Pax6. (A) EGFP reporter allele reveals Cre recombinase activity within the prethalamus and ventral telencephalon of Gsx2^{Cre} embryos at E14.5. Staining for L1 shows the position of the thalamocortical tract. **B)** Immunohistochemistry showing

Pax6 expression. Note that Pax6 expression in the prethalamus is similar to prethalamic Gsx2 expression pattern shown in image A. **C)** EGFP reporter allele revealing Cre activity in Zic4^{Cre} embryos at E13.5 and thalamocortical axons expressing L1. **D)** High power image showing the absence of axonal projections from Zic4-lineage prethalamic cells towards the thalamus. **E-E'')** Neurons belonging to the Gsx2 lineage extend parallel projections across the thalamus in close apposition to L1-positive thalamocortical axons. E' and E'' are a higher magnification of the area framed in E. **F-H)** Injection of the tracer Neurobiotin in the thalamus at E13.5 resulted in the retrograde labelling of neurons in the prethalamus (arrow in F). F-G: Prethalamic labelled neurons belong to the Gsx2 lineage shown by GFP immunohistochemistry combined with Neurobiotin visualization. F and F' are separate channels from image F''. G is a zoom of the framed area in F''. H,H': Parallel section of F'' processed for Pax6 immunoshistochemistry combined with Neurobiotin visualization showing that most prethalamic neurobiotin-positive neurons are also Pax6 positive (arrows). **I)** Schematic summary. Scale bars: 500µm (A,B,C,E), 250µm (F), 100µm (D, E',G,H). Ctx= cortex, Nb= Neurobiotin, Pth= prethalamus, Th= thalamus, vTel= ventral telencephalon,

Figure 4. Disruption of prethalamic pioneer axons in Gsx2^{Cre} Pax6 cKOs causes abnormal fasciculation but not changes in topography. A-F) Prethalamic pioneer axons visualized by EGFP reporter in Gsx2^{Cre} embryos are reduced in Gsx2^{Cre} Pax6 cKOs at E12.5 (A,B), E13.5 (C,D) and E14.5 (E,F) **G-J)** Use of the DTy54 YAC reporter allele, which labels cells in which the *Pax6* gene is active, also reveals a reduction in prethalamic pioneer axons crossing the thalamus. **K,L)** Injection of the tracer DiI in the thalamus of E13.5 retrogradelly labels cell bodies in the prethalamus of controls (arrow in K) but not in CAG^{CreER} Pax6 cKOS

(L). Inset in K is a fluorescent immunohistochemistry for Pax6 combined with DiI visualization showing that the DiI-labelled prethalamic neurons are expressed in the Pax6 positive area. **M-N)** Immunofluorescence for L1 shows formation of abnormal big bundles of thalamocortical axons crossing the prethalamus in $Gsx2^{Cre}$ Pax6 cKOs (arrow in N,P,R) with respect to controls (M,O,Q) at E14.5 (M,N), E16.5 (O,P) and E18.5 (Q,R). **S)** DiI and DiA injection in the cortex of $Gsx2^{Cre}$ pax6 cKO embryos shows that the topography of TCAs is not affected in these mutants. **T)** Schematic summary. Scale bars: 250µm (G,H,S), 100 µm (A-F, I-P). Ctx= cortex, Pth= prethalamus, TCA= thalamocortical axons, Th= thalamus, vTel= ventral telencephalon.

Figure 5. Subsets of thalamocortical axons show a preference to navigate through different parts of the thalamus. A,B) Immunohistochemistry for L1 shows that thalamocortical axons exhibit disorganized and erroneous trajectories in the thalamus of E13.5 CAG^{CreER} Pax6 cKOs (B) with respect to controls (A). Arrow in B points to one big bundle deviating from lateral to medial thalamus. **C-J)** Schemas and images of the transplants using lateral (C-F) or medial (G-J) donor thalamus and grafted into lateral (C,D,G,H) or medial (E,F,I,J) host tissue. Images show immunofluorescence for GFP and Pax6. Lateral axons show a strong preference to navigate through lateral thalamus (C-F) while medial axons show a more variable response (G,J). Empty arrows in H and J point to a medial corridor through which many medial axons preferentially navigate. White arrows in J show medial axons turning from lateral to medial regions of the thalamus. Scale bars: 100µm. Ctx= cortex, Pth= prethalamus, Th= thalamus, vTel= ventral telencephalon.

**Figure 6. Axon guidance molecules and their receptors are altered in the diencephalon of CAG^{CreER} Pax6 cKOs. A-I') ** Expression pattern of *Ntn1* and

895 *Sema3a* mRNA and their receptors *Unc5c* and *Plxna1* in the E13.5 diencephalon of
896 controls (A-E') and CAG^{CreER} Pax6 cKOs (F-I'). C and H show two views of 3D
897 reconstructions of the expression pattern of *Ntn1* and *Sema3a* from transverse ISH
898 sections. For each panel, the 3D model show on the left is a frontal view in the same
899 plane of a transverse section while the one on the right (medial view) is a view from
900 the ventricular surface. **J,K)** Schematic model of the changes in *Ntn1* and *Sema3a*
901 expression in the thalamus of controls (J) versus CAG^{CreER} Pax6 cKOs (K) and how
902 we hypothesize might affect the guidance of different subsets of thalamic axons. In
903 controls (J), lateral thalamic neurons express Unc5c and Plxna1, therefore are
904 repelled by both guidance cues, which direct their axons out from the thalamus and
905 towards the prethalamus in a straight trajectory. In Pax6 cKOs (K) some lateral
906 thalamic neurons lose their *Unc5c* expression but maintain their *Plxna1* expression,
907 therefore losing their repulsion to *Ntn1* but maintaining it for *Sema3a*. This makes
908 their axons deviate towards medial thalamic regions. Scale bars: 500µm (A,B,D-
909 E,F,G,I,J), 100µm (D',I'). Ctx= cortex, Pth= prethalamus, Th= thalamus, vTel= ventral
910 telencephalon.

911

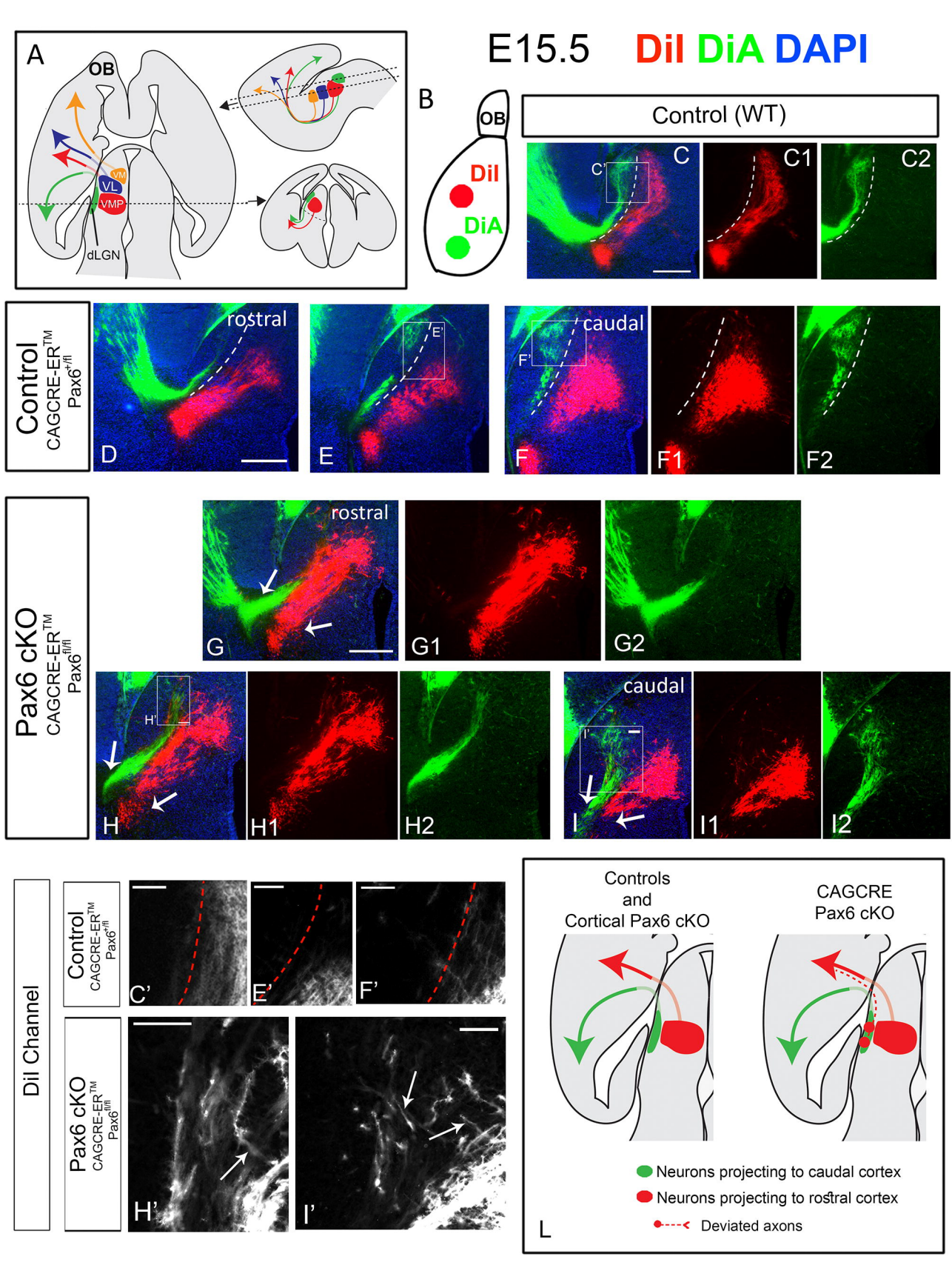
A
OB
VM
VL
VMP
dLGN
B
OB
Dil
DiA
E15.5 Dil DiA DAPI
Control (WT)
C
C'
C1
C2
Control
CAGCRE-ER^TM
Pax6^+/fl
rostral
caudal
D
E
E'
F
F'
F1
F2
Pax6 cKO
CAGCRE-ER^TM
Pax6^fl/fl
G
G1
G2
H
H'
H1
H2
I
I'
I1
I2
Dil Channel
Control
CAGCRE-ER^TM
Pax6^+/fl
C'
E'
F'
Pax6 cKO
CAGCRE-ER^TM
Pax6^fl/fl
H'
I'
Controls
and
Cortical Pax6 cKO
CAGCRE
Pax6 cKO
Neurons projecting to caudal cortex
Neurons projecting to rostral cortex
Deviated axons
L

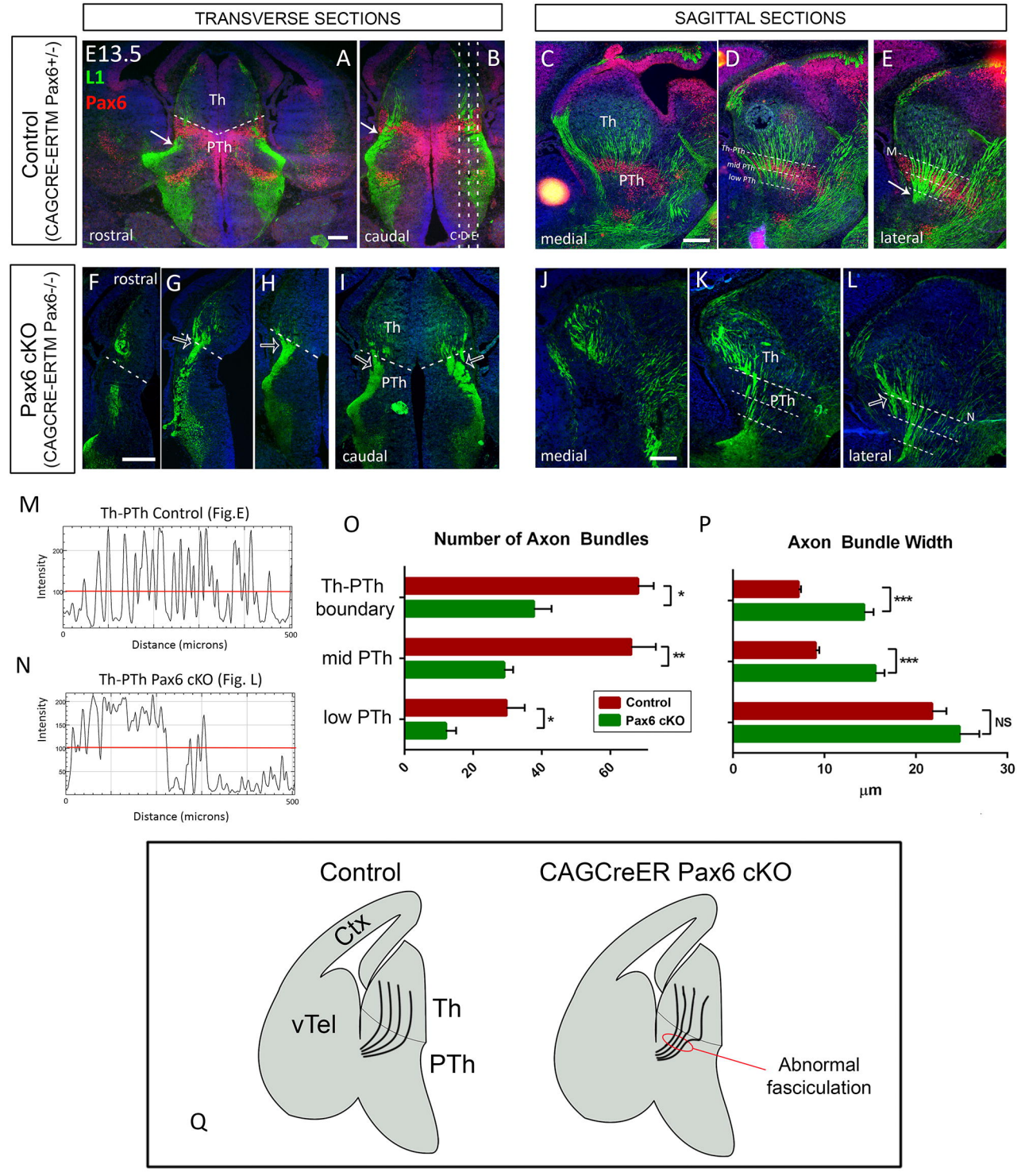
TRANSVERSE SECTIONS
SAGITTAL SECTIONS
Control
(CAGCRE-ERTM Pax6+/-)
E13.5
L1
Pax6
A
B
Th
PTh
rostral
caudal
C D E
C
D
E
Th
PTh
medial
Th-PTh
mid PTh
low PTh
M
lateral
Pax6 cKO
(CAGCRE-ERTM Pax6-/-)
F rostral
G
H
I
Th
PTh
caudal
J
K
L
medial
Th
PTh
N
lateral
M
Th-PTh Control (Fig.E)
Intensity
Distance (microns)
N
Th-PTh Pax6 cKO (Fig. L)
Intensity
Distance (microns)
O
Number of Axon Bundles
Th-PTh boundary
mid PTh
low PTh
*
**
*
Control
Pax6 cKO
0
20
40
60
P
Axon Bundle Width
***
***
NS
0
10
20
30
µm
Q
Control
CAGCreER Pax6 cKO
Ctx
vTel
Th
PTh
Abnormal fasciculation

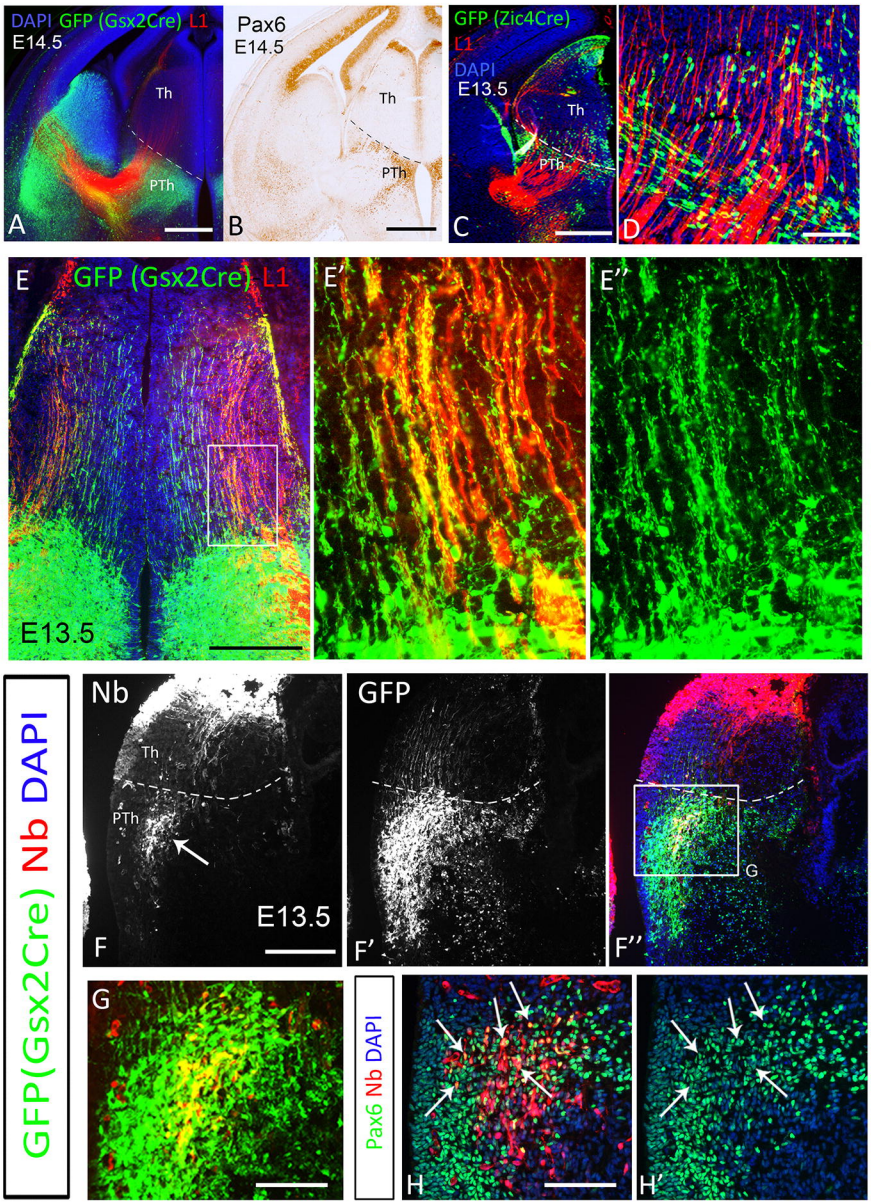
DAPI GFP (Gsx2Cre) L1
E14.5
Th
PTh
A
Pax6
E14.5
Th
PTh
B
GFP (Zic4Cre)
L1
DAPI
E13.5
Th
PTh
C
D
E
GFP (Gsx2Cre) L1
E13.5
E'
E''
GFP(Gsx2Cre) Nb DAPI
Nb
Th
PTh
E13.5
F
GFP
F'
G
F''
G
Pax6 Nb DAPI
H
H'
Ctx
vTel
Th
PTh
PRETHALAMIC
PIONEER NEURONS
Gsx2 lineage
Pax6 positive
I

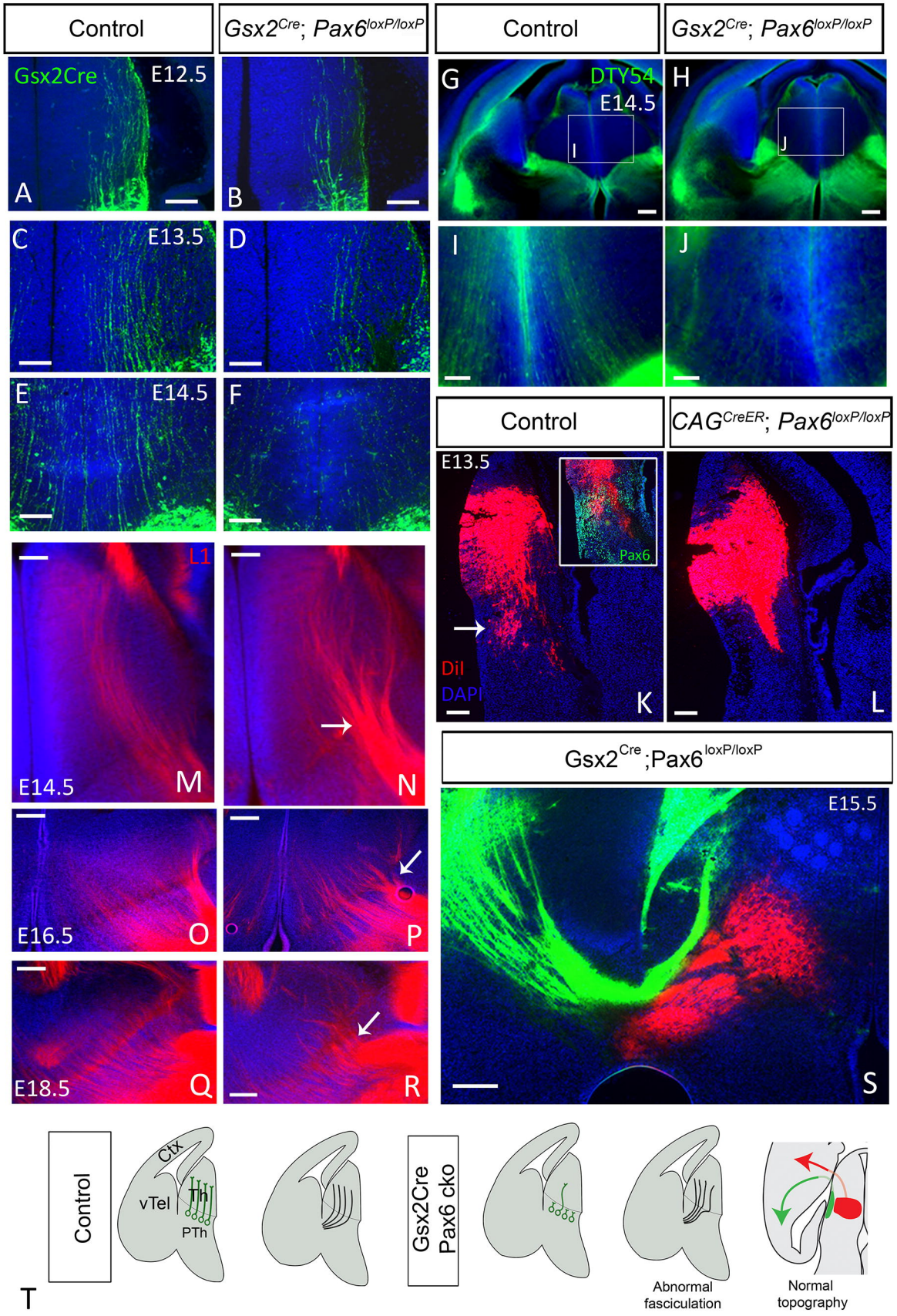
Control
Gsx2Cre; Pax6loxP/loxP
Control
Gsx2Cre; Pax6loxP/loxP
Gsx2Cre
E12.5
A
B
G
DTY54
E14.5
I
H
J
C
E13.5
D
I
J
E
E14.5
F
Control
CAGCreER; Pax6loxP/loxP
L1
E13.5
Pax6
DiI
DAPI
K
L
E14.5
M
N
Gsx2Cre;Pax6loxP/loxP
E15.5
E16.5
O
P
E18.5
Q
R
S
T
Control
Ctx
vTel
Th
PTh
Gsx2Cre
Pax6 cko
Abnormal
fasciculation
Normal
topography

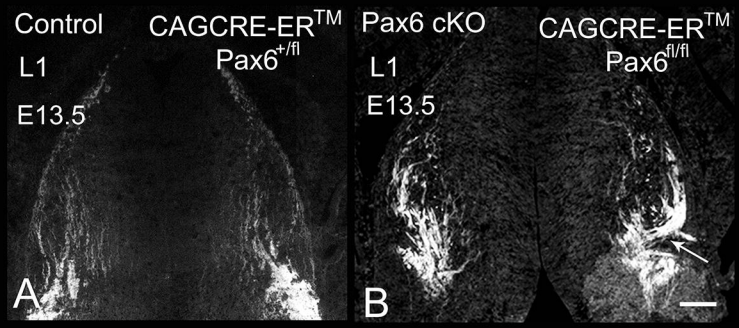
Control
CAGCRE-ER^{TM}
Pax6$^{+/fl}$
L1
E13.5
A
Pax6 cKO
CAGCRE-ER^{TM}
Pax6$^{fl/fl}$
L1
E13.5
B

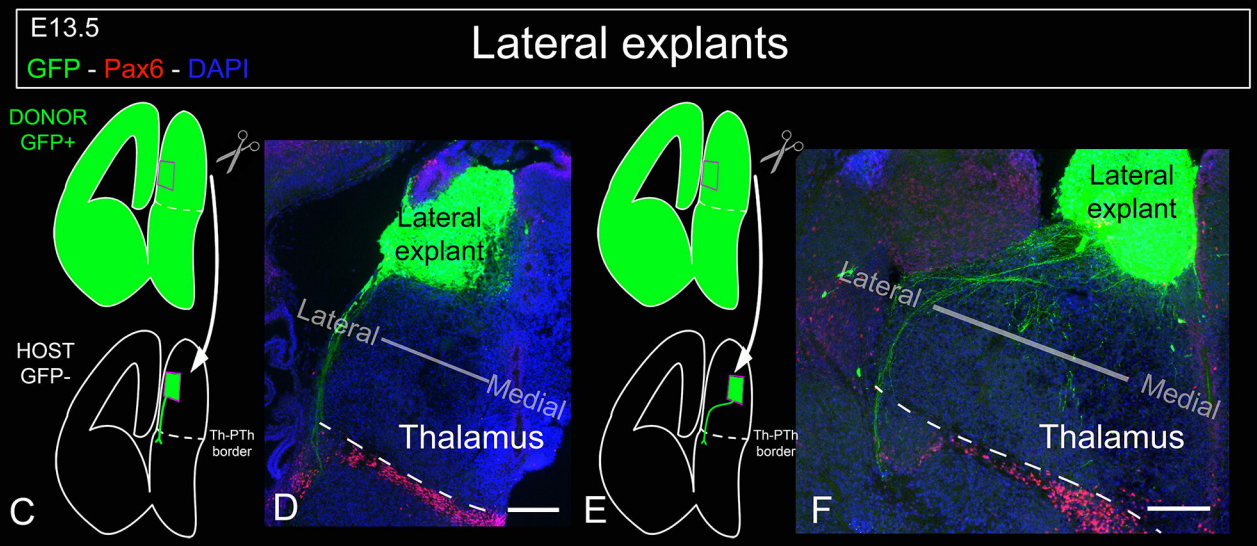
E13.5
GFP - Pax6 - DAPI
Lateral explants
DONOR
GFP+
HOST
GFP-
Th-PTh
border
C
Lateral
explant
Lateral
Medial
Thalamus
D
Th-PTh
border
E
Lateral
explant
Lateral
Medial
Thalamus
F

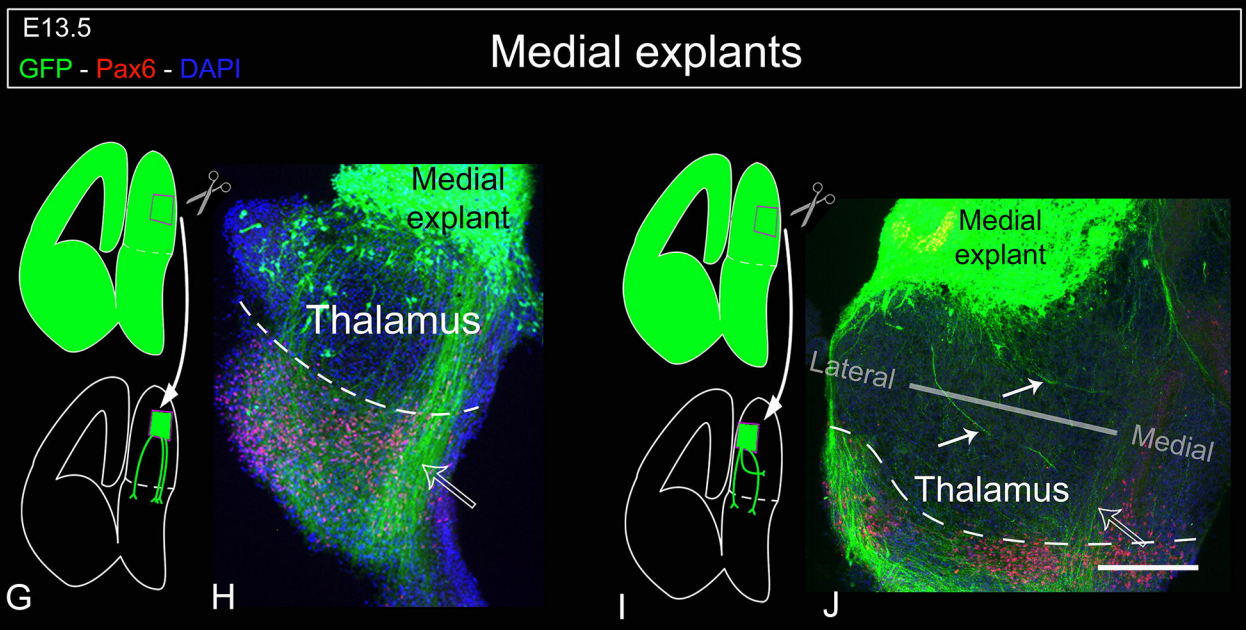
E13.5
GFP - Pax6 - DAPI
Medial explants
Medial
explant
Thalamus
G
H
Medial
explant
Lateral
Medial
Thalamus
I
J

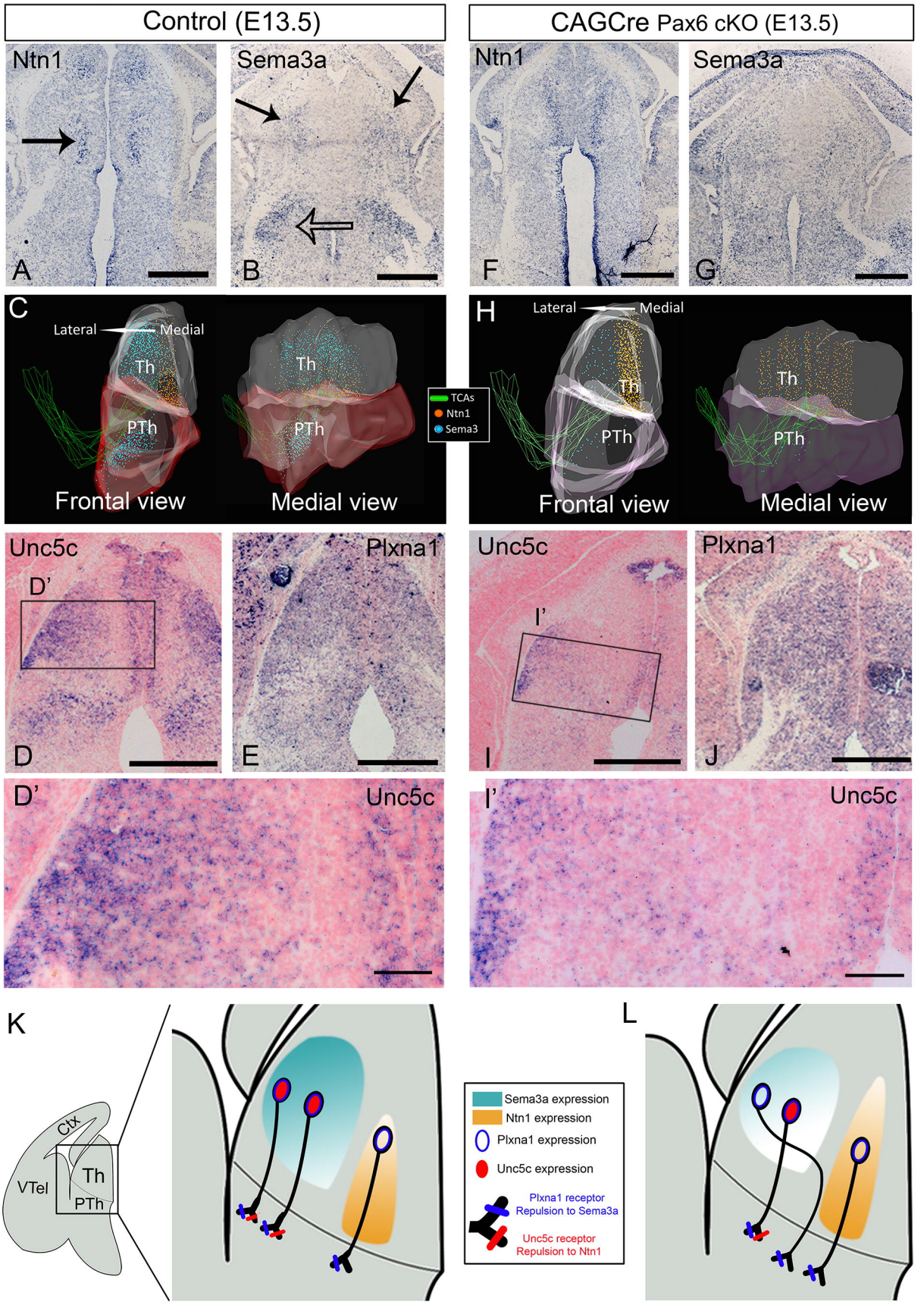
Control (E13.5)
CAGCre Pax6 cKO (E13.5)
Ntn1
Sema3a
Ntn1
Sema3a
A
B
F
G
C
Lateral
Medial
Th
PTh
Frontal view
Medial view
TCAs
Ntn1
Sema3
H
Lateral
Medial
Th
PTh
Frontal view
Medial view
Unc5c
D'
Plxna1
Unc5c
I'
Plxna1
D
E
I
J
D'
Unc5c
I'
Unc5c
K
Ctx
VTel
Th
PTh
Sema3a expression
Ntn1 expression
Plxna1 expression
Unc5c expression
Plxna1 receptor
Repulsion to Sema3a
Unc5c receptor
Repulsion to Ntn1
L